Global Water Availability and Requirements for Future Food Production

D. GERTEN AND J. HEINKE

Potsdam Institute for Climate Impact Research, Research Domain of Climate Impacts and Vulnerabilities, Potsdam, Germany

H. HOFF

Potsdam Institute for Climate Impact Research, Research Domain of Climate Impacts and Vulnerabilities, Potsdam, Germany, and Stockholm Environment Institute, Stockholm, Sweden

H. BIEMANS

Wageningen University and Research Centre, Earth System Science and Climate Change, Wageningen, Netherlands

M. FADER

Potsdam Institute for Climate Impact Research, Research Domain of Climate Impacts and Vulnerabilities, Potsdam, and International Max Planck Research School on Earth System Modelling, Hamburg, Germany

K. WAHA

Potsdam Institute for Climate Impact Research, Research Domain of Earth System Analysis, Potsdam, Germany

ABSTRACT

This study compares, spatially explicitly and at global scale, per capita water availability and water requirements for food production presently (1971–2000) and in the future given climate and population change (2070–99). A vegetation and hydrology model Lund–Potsdam–Jena managed Land (LPJmL) was used to calculate green and blue water availability per capita, water requirements to produce a balanced diet representing a benchmark for hunger alleviation [3000 kilocalories per capita per day (1 kilocalorie = 4184 joules), here assumed to consist of 80% vegetal food and 20% animal products], and a new water scarcity indicator that relates the two at country scale. A country was considered water-scarce if its water availability fell below the water requirement for the specified diet, which is presently the case especially in North and East Africa and in southwestern Asia. Under climate (derived from 17 general circulation models) and population change (A2 and B1 emissions and population scenarios), water availability per person will most probably diminish in many regions. At the same time the calorie-specific water requirements tend to decrease, due mainly to the positive effect of rising atmospheric CO_2 concentration on crop water productivity—which, however, is very uncertain to be fully realized in most regions. As a net effect of climate, CO_2, and population change, water scarcity will become aggravated in many countries, and a number of additional countries are at risk of losing their present capacity to produce a balanced diet for their inhabitants.

1. Introduction

Comprehensive knowledge of how freshwater availability and scarcity will evolve in the future in response to climatic and socioeconomic changes is of tremendous importance for all water-dependent sectors and especially for agriculture (Molden 2007; Bates et al. 2008). For this reason, one objective of the Water and Global Change (WATCH) project is not just to assess the potential future changes in the terrestrial water balance per se (evapotranspiration and runoff) but also to put these changes into the context of, for example, global food production given demographic changes in addition

to climatic changes. Until recently, most assessments and projections of worldwide water resources (Vörösmarty et al. 2000; Arnell 2004; Alcamo et al. 2007; Islam et al. 2007) were focused on the "blue" water (BW) of rivers, lakes, reservoirs, and aquifers. However, it is "green" water (GW)—the precipitation water that infiltrates into the soil (Falkenmark et al. 2009)—that sustains the growth and productivity of all terrestrial ecosystems and makes up most of the water consumption in agriculture (Rost et al. 2008; Liu et al. 2009). Therefore, both green and blue water need to be included in water availability and scarcity analyses. An integrated assessment of both GW and BW resources has been initiated only recently by use of macroscale hydrological, ecological, and crop models [Liu et al. 2007, 2009; Rost et al. 2008; Schuol et al. 2008; Weiß et al. 2009; Siebert and Döll 2010; see also Hoff et al. (2010) for an overview and a synthesis of recent efforts].

Nevertheless, it remains a conceptual challenge how to clearly define the GW resource and how to represent it consistently with BW in generic indicators of water availability and scarcity such as the widely used Falkenmark Index that relates water resources to population. In the global-scale study of Rockström et al. (2009), a first variant of such an enhanced water scarcity indicator was developed. Those authors defined the GW resource as the total evapotranspiration (ET; sum of plant transpiration, soil evaporation, and interception losses) that occurs from grazing land and cropland (including the non-BW fraction on irrigated areas) in a country, and they related this GW resource to the country population. If the value of this modified Falkenmark index that combines GW and BW fell below 1300 cubic meters per capita per year, green-blue water scarcity was assumed to prevail. Note that the threshold for chronic water scarcity was set to a higher value (as compared to 1000 cubic meters per capita per year if only blue water is considered) in order to account preliminarily for the additional resource (i.e., the green water). Rockström et al. (2009) found that in stark contrast to studies based solely on an estimation of BW resources, actually only a few regions are presently categorized as water-scarce if GW is also taken into account. However, they also found that under conditions of future climate and population change [Special Report on Emissions Scenarios (SRES) A2, the second climate configuration of the Met Office Unified Model (HadCM2)], many countries in northern Africa, the Near East, and southern Asia will turn to a water-scarce status.

Further, Rockström et al. (2009) assumed that countries with less than 1300 cubic meters per capita per year of total green and blue water resources cannot produce a balanced diet of 3000 kilocalories per capita per day [1 kilocalorie (kcal) = 4184 joules (J)] with shares of 80% vegetal and 20% animal products, which can be regarded as a benchmark for hunger alleviation (Rockström et al. 2007). This national average calorie level was chosen as a desirable baseline in the present study, since previous analyses found that the number of undernourished people in a country approaches zero only when the average diet reaches ~3000 kilocalories per capita per day (Rockström et al. 2005); this value also is the average calorie level projected by the Food and Agriculture Association (FAO) to be reached in developing countries by 2030 (FAO 2003). We note that present diets differ from it in many countries—for example, exceeding 3700 kilocalories per capita per day (27% share of animal products) in North America and falling below 2500 kilocalories per capita per day (<8% share of animal products) in many African countries (see http://faostat.fao.org/site/609/default.aspx#ancor).

While the abovementioned threshold of 1300 cubic meters water per person needed to produce 3000 kilocalories per capita per day may be valid as a global average, significantly more—or less—water is required in individual regions for producing that diet. The main reason is that the crop water productivity (CWP)—the ratio between crop yield and ET during the growing period—differs significantly among regions because of differences in climatic and management conditions. For instance, CWP was found to be significantly lower in sub-Saharan Africa than in northern Europe (Liu et al. 2007; Fader et al. 2010). Hence, using the global average threshold would underrate water scarcity for regions where in fact >1300 cubic meters per capita per year is needed for producing the specified diet, and vice versa.

This study quantifies the GW and BW availabilities for each country of the world and directly compares these to the water requirements for producing a diet of 3000 kilocalories per capita per day (with 80% vegetal products) calculated from local crop water productivities. The resulting new water scarcity indicator is applied for both the present situation and for a large number of global change scenarios [climate change from 17 general circulation models (GCMs), including direct CO_2 effects on plants; B1 and A2 emissions and population scenarios]. All calculations were done at high spatial resolution (0.5° global grid, separately for rain-fed and irrigated areas) and also at high temporal resolution (daily time step, transient simulation from 1901 to 2099), while results are presented as 30-yr country averages (blending results for rain-fed and irrigated land) for the present (1971–2000) and for a future time slice (2070–99 or "2080s"), respectively.

2. Model and methods

In the following we will briefly present the model used for our calculations (section 2a); describe how the blue, green, and joint green-blue water resources and availabilities per capita were computed at grid cell level and how they were then scaled to the country level (section 2b); and, finally, show how the water requirements for producing the balanced diet were computed at grid cell level for both cropland and a hypothetical livestock sector, and how these requirements were scaled to country level (section 2c). Section 2b also describes how the new water scarcity was derived at country scale by relating the green-blue water availability to the water requirements.

a. The LPJmL dynamic global vegetation and water balance model

For this study the process-based, global ecohydrological model Lund–Potsdam–Jena managed Land (LPJmL) was applied, which has a proven capability for simulating GW and BW resources, crop–water interactions, and their temporal dynamics (Gerten et al. 2008; Rost et al. 2008; Biemans et al. 2009; Fader et al. 2010). The model simulates the growth, production, and phenology of nine "plant functional types" (PFTs, representing natural vegetation at the level of biomes), grazing land, and 12 "crop functional types" [CFTs, representing the world's major food crops as described in Bondeau et al. (2007): temperate and tropical cereals, rice, maize, pulses, temperate and tropical roots, sunflower, soybean, groundnuts, rapeseed, and a heterogeneous group of "other" crops collectively parameterized like perennial grasses]. While the composition and distribution of the PFTs was simulated by the model, the fractional coverage of grid cells with CFTs was prescribed. In short, we combined a dataset of the present (around year 2000) cropland distribution (Ramankutty et al. 2008) with a dataset of maximum monthly irrigated and rain-fed harvested areas of 26 crops (Portmann et al. 2010) that we aggregated to the CFTs (see Fader et al. 2010). The fractions of CFTs and grazing land were held constant at the year 2000 level throughout the simulation period (also in the past) in order to minimize effects of factors other than climate and population.

Carbon fluxes and pools as well as water fluxes (evaporation from soils, vegetation canopies, water bodies, and irrigation channels; transpiration; soil moisture dynamics; snowmelt; runoff and discharge; return flow from irrigated sites) are modeled in direct coupling with vegetation dynamics. Atmospheric CO_2 concentration directly affects transpiration and biomass production via both physiological and structural plant responses, which as a net effect tend to reduce the amount of water transpired per unit of biomass produced (Leipprand and Gerten 2006; Gerten et al. 2007).

Water requirements and water consumption—and thereby the CWP—of irrigated and rain-fed CFTs are distinguished, with an explicit distinction of GW and BW contributions on irrigated land. We assumed that the irrigation water requirements of the CFTs—as controlled by their water limitation and by country-wide irrigation efficiencies—can always be fulfilled (see Rost et al. 2008). River flow directions were determined as in the WATCH–Global Water System Project (GWSP) Model Intercomparison Project (WaterMIP) simulation protocol (Haddeland et al. 2011). See below for details on the modeling of GW and BW availability.

Seasonal phenology (sowing and harvest dates) of CFTs was simulated based on CFT-specific parameters, past climate and current meteorological conditions, allowing for adaptation of varieties and growing periods to climate change (Bondeau et al. 2007; Waha et al. 2011). To ensure sound estimates of CFT yields and water productivities, yields were calibrated for the period around 2000 against those reported in the Food and Agriculture Organization's FAOSTAT database (http://faostat.fao.org/site/567/DesktopDefault.aspx?PageID=567#anc) by sequentially varying parameters for cropping density and other management-related features [calibration procedure as in Fader et al. (2010), but with the here used model version; that study and also Fader et al. (2011) demonstrate that yields and crop water productivities agree well with other estimates]. The calibration parameters, the irrigation efficiencies, and the fractional coverage of irrigated and rain-fed cropland and grazing land were held constant at their year 2000 value for the future period. Thus, it was assumed that neither changes in crop and water management nor changes in the extent of agricultural land will occur in the future.

The present model version (LPJmL_v3.2) is an upgrade of the version documented by Rost et al. (2008) and Fader et al. (2010), including a revised representation of crop phenology (Waha et al. 2011) and a reservoir management scheme (Biemans et al. 2011).

b. Calculation of blue water and green water resources and availability

The BW resource (runoff) and the GW resource (ET from cropland and grazing land; both in $m^3 \ yr^{-1}$) were computed at the grid cell level and then summed up for the respective country. The assumption underlying this calculation procedure is that the food produced with this water is distributed evenly within a country rather than produced and consumed within individual grid cells or within a river basin.

1) BLUE WATER RESOURCE

For determining the BW resource we first computed, for the zero-order river basins of the globe, the runoff R generated (assuming no withdrawals from lakes and reservoirs) in each 0.5° grid cell located within the basin boundaries (i) and summed these values up to yield the total runoff generated in a basin R_b.

Second, we redistributed R_b across the basin in proportion to the share of a cell's discharge Q (accumulated along the river network) relative to the discharge sum of all cells in a basin:

$$BW_i = R_b Q_i \Big/ \sum Q_i, \qquad (1)$$

where BW_i represents the blue water resource (i.e., redistributed runoff) in each grid cell i. This way, grid cells with a high discharge were assigned a relatively high BW resource. Runoff distributed this way across the basin was used instead of discharge in order to avoid double counting of water passing more than one cell.

Third, the BW resource per country was derived by summing up the thus determined values of BW_i for all grid cells in the country. It was furthermore assumed that only 40% of this resource is actually available for food production, to account collectively (without explicit separation in individual components) for environmental flow requirements and for the fact that the spatiotemporal variability of BW resources often does not match the demand. Moreover, use of 40% or more of blue water resources is a widely accepted indicator of water stress (e.g., Vörösmarty et al. 2000). Note that water consumption by households and industry was not considered here, such that the BW resource is somewhat overestimated where this consumption is significant (especially in industrialized countries; globally, however, water consumption in these sectors is by far lower than agricultural consumption).

2) GREEN AND GREEN-BLUE WATER RESOURCE

The volumetric GW resource of a country is defined here as the green water consumed (evapotranspired) on cropland and grazing land. On rain-fed areas, it equals total ET; on irrigated areas, it equals total ET minus ET of blue irrigation water [see Rost et al. (2008) on how the individual contributions of green and blue water in the soil are computed by LPJmL]. Only 50% of ET was considered from areas covered with perennial "other" crops (see above) because those crops actually grow only during part of the year, and because nonfood crops (cotton in particular) are included in this category. The GW contribution from grazing land is driven by demand for grazing and thus was constrained either by total

grassland ET or by the global average water requirement of 251 cubic meters per capita per year from grazing land as calculated below. In our provisional treatment (subject to further improvements) of the livestock sector, we have preferred this approach over the use of country-specific estimates of GW consumption on grazing land (in case total grassland ET was higher than the global average), because the management of grazing land is only crudely represented in LPJmL (emulating mowing intervals only; see Bondeau et al. 2007). Since grassland is usually managed in a different way than cropland, using the (area-corrected) value of ET from cropland in the respective country as a proxy for ET from grazing land was not suitable either. Note that the GW resource also reflects the extent of agricultural area, such that countries with a large agricultural area may show a relatively high GW resource; this is often true for dry regions that compensate for low water availability by extensive agriculture.

The total green and blue water resource GWBW ($m^3 \ yr^{-1}$) is calculated as the sum of the GW and BW resources in a country.

3) BLUE AND GREEN-BLUE WATER AVAILABILITY AND SCARCITY

BW availability and GWBW availability (both in cubic meters per capita per year) were determined by relating the annual BW (and, respectively, GWBW) resource to the number of people living in a country. This way, people were assumed to benefit uniformly across the respective country from its total water resource rather than only from the resource within the grid cell where they live. GWBW scarcity—the new water scarcity indicator introduced in this paper—was computed for each country as the ratio between the GWBW availability and the water requirement for producing the balanced diet (described in the following).

c. Calculation of dietary water requirements

The countries' water requirements for producing a diet of 3000 kilocalories per capita per day with 20% calories from animal products was estimated from both the water requirements to produce vegetal calories on a country's present cropland (represented by the 12 CFTs) and from a hypothetical livestock sector (the water consumption of which was computed from grazing land and cropland for feed production). The calculation principle is illustrated in Fig. 1 and described in the following.

The water needs for the vegetal part were estimated by calculating the total amount of calories produced on a grid cell's cropland (inferred from simulated production using global average calorie conversion factors
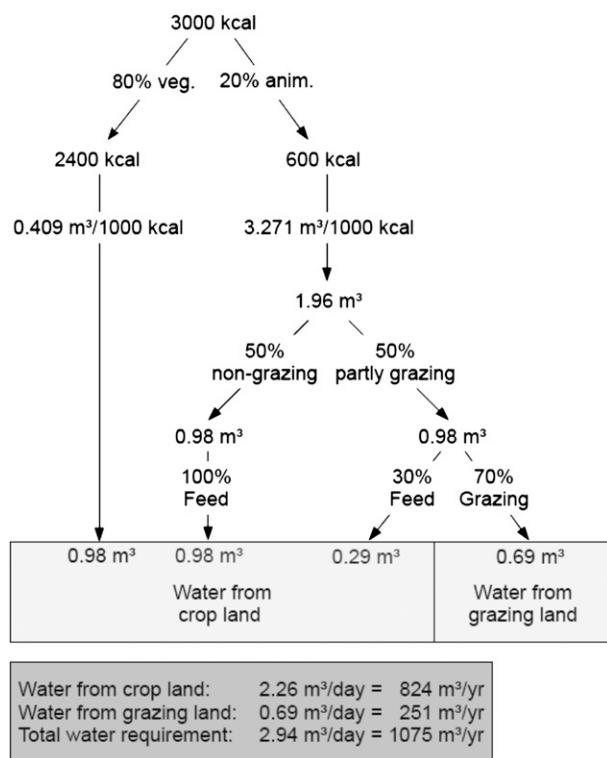
FIG. 1. Calculation scheme for water requirements from cropland and grazing land, and LPJmL-computed global values (1971–2000 average) for the individual components. Figure reproduced after Lannerstad (2009).

(g dry matter to kcal) based on the FAO's Food Balance Sheets for primary commodities (http://faostat.fao.org/site/368/default.aspx#ancor) and relating it to the total amount of GWBW consumed on cropland during the growing period. The estimated global requirement of 0.409 m^3 (1000 kcal)$^{-1}$ [=0.98 m^3 (2400 kcal)$^{-1}$] broadly confirms the 0.5 m^3 (1000 kcal)$^{-1}$ estimated by Rockström et al. (2007) based on statistical data. Following those authors, the eightfold amount of water is required to produce an equivalent amount of animal calories [3.271 m^3 (1000 kcal)$^{-1}$ = 1.96 m^3 (600 kcal)$^{-1}$] (see Fig. 1). This is an indicative guess (from Table 1 in Rockström et al. 2007) based on the fact that more water is required to produce a calorie of animal-based food because only a fraction (~5%–15%) of the vegetal energy consumed by animals is transformed into meat, milk, or eggs. This calculation results in a global average of 1075 cubic meters of water per capita and year required for the above specified diet (358 cubic meters per capita per year for the vegetal share plus 716 cubic meters per capita per year for the animal share), which is accordingly lower than the 1300 cubic meters per capita per year estimated by Rockström et al. (2007, 2009).

The water requirements to produce the animal share of the diet were attributed to cropland and grazing land assuming a mixed livestock system with a nongrazing and a partly grazing subsystem, each consuming 50% of the water (Rockström et al. 2007; Lannerstad 2009). The nongrazing system entirely relies on feed produced on cropland, whereas in the partly grazed system 30% of the water was assumed to be required to produce feed on cropland and the remainder was assigned to grazing land. As a result, 824 cubic meters per capita per year (out of the total 1075 cubic meters per capita per year) are required to produce food and feed on cropland, and 251 cubic meters per capita per year are required to produce grazed biomass. It can also be inferred that 56% (466 cubic meters per capita per year) of the water required on cropland is used to produce animal feed.

For individual countries, the GWBW amount required to produce food and feed on cropland was computed as above from the country-specific requirement to produce 1000 kcal. For the water requirements from grazing land we simply used for each country the global average of 251 cubic meters per capita per year, arguing that grassland management and grazing intensity are not related to cropland productivity. In a simple sensitivity analysis, we also quantified the effect of a reduction of the diet's share of animal products from 20% to 10% (meaning that more food and thereby water is consumed from cropland and less from grassland). For all future projections, the country-specific share of the water resource from grazing land was held constant at the present level.

3. Climate data and scenarios

LPJmL was forced for the period 1901–2000 by monthly values of air temperature, precipitation amounts, number of wet days, and cloud cover, taken from the Climate Research Unit time series (CRU TS) 3.0 climate database (Mitchell and Jones 2005; http://badc.nerc.ac.uk/data/cru/). Prior to running the model, these data were disaggregated to daily values using stochastic procedures, as in Gerten et al. (2004). In a 1000-yr spinup simulation, the climate of 1901–30 was repeatedly run to equilibrate the carbon pools and the natural vegetation. Soil parameters and historical annual atmospheric CO_2 concentrations were as in Rost et al. (2008).

Climate projections for the subsequent transient simulations up to the year 2099 were derived from 17 GCMs under forcing from the SRES A2 and B1 emissions scenario (those models were chosen for which both B1 and A2 projections were available). All GCMs participated in the World Climate Research Programme's Coupled Model Intercomparison Project phase 3 (CMIP3; http://www-pcmdi.llnl.gov/projects/cmip/index.php) and

TABLE 1. GCMs considered in this study [see Randall et al. (2007) for details].

GCM	Sponsor(s), country
Bjerknes Centre for Climate Research Bergen Climate Model version 2 (BCCR-BCM2.0)	Bjerknes Centre for Climate Research, Norway
Community Climate System Model, version 3 (CCSM3)	National Center for Atmospheric Research (NCAR), United States
Canadian Centre for Climate Modelling and Analysis (CCCma) Coupled General Circulation Model, version 3.1 (CGCM3.1)	Canadian Centre for Climate Modeling and Analysis, Canada
Centre National de Recherches Météorologiques Coupled Global Climate Model, version 3 (CNRM-CM3)	Météo-France/Centre National de Recherches Météorologiques, France
Commonwealth Scientific and Industrial Research Organisation Mark version 3.0 and 3.5 (CSIRO-MK3.0 and -MK3.5)	Commonwealth Scientific and Industrial Research Organization, Atmospheric Research, Australia
ECHAM5/Max Planck Institute Ocean Model (MPI-OM)	Max Planck Institute for Meteorology, Germany
ECHAM and the global Hamburg Ocean Primitive Equation (ECHO-G)	Meteorological Institute of the University Bonn, Meteorological Research Institute of the Korea Meteorological Administration (KMA), and Model and Data Group, Germany/Korea
Geophysical Fluid Dynamics Laboratory Climate Model versions 2.0 and 2.1(GFDL-CM2.0 and -CM2.1)	U.S. Department of Commerce/National Oceanic and Atmospheric Administration (NOAA)/Geophysical Fluid Dynamics Laboratory (GFDL), United States
Goddard Institute for Space Studies Model E-R (GISS-ER)	National Aeronautics and Space Administration (NASA)/ Goddard Institute for Space Studies (GISS), United States
Institute of Numerical Mathematics Coupled Model, version 3.0 (INM-CM3.0)	Institute for Numerical Mathematics, Russia
L'Institut Pierre-Simon Laplace Coupled Model, version 4 (IPSL-CM4)	Institut Pierre Simon Laplace, France
Model for Interdisciplinary Research on Climate 3.2, medium-resolution version [MIROC3.2(medres)]	Center for Climate System Research (University of Tokyo), National Institute for Environmental Studies, and Frontier Research Center for Global Change (JAMSTEC), Japan
Meteorological Research Institute Coupled General Circulation Model, version 2.3.2a (MRI-CGCM2.3.2)	Meteorological Research Institute, Japan
Parallel Climate Model (PCM)	NCAR, United States
Third climate configuration of the Met Office Unified Model (UKMO-HadCM3)	Hadley Centre for Climate Prediction and Research/Met Office, United Kingdom

were used in the Intergovernmental Panel on Climate Change (IPCC) Fourth Assessment Report (Randall et al. 2007; see Table 1). The climate scenarios were prepared as follows.

First, the individual GCMs' monthly mean air temperatures, precipitation sums, and mean cloudiness values were interpolated to 0.5° resolution and smoothed using a 30-yr running mean with a minimum roughness constraint at the 2099 boundary (Mann 2004). Then, anomalies relative to the 1971–2000 average were calculated for each GCM and month of the 2001–99 period and applied to the observed 1971–2000 baseline climate (continuously repeated after 2000 while preserving the variability of the observations). In the case of temperature, the anomalies were simply added, as follows:

$$T_{\text{scl}} = T_{\text{obs}} + T_{\text{ano}}, \qquad (2)$$

where T_{scl} is the scaled monthly value of the GCM scenario (e.g., January 2001), and T_{obs} is the monthly

value of the observed baseline time series (January 1971 in this example). Here T_{ano} is the anomaly within the original GCM runs—that is, the difference between the GCM-simulated mean temperature in a given month (e.g., January 2001) and the GCM-simulated 30-yr monthly average for the 1971–2000 baseline period ($Tm_{\text{bas\_sim}}$):

$$T_{\text{ano}} = T_{\text{sim}} - Tm_{\text{bas\_sim}}. \qquad (3)$$

For cloudiness (in %), decreases and increases were applied as a relative change of cloudiness and cloudlessness, respectively. If cloudiness C decreases in the GCM simulation relative to the baseline average (i.e., if $C_{\text{ano}} < 0$), we assume

$$C_{\text{scl}} = C_{\text{obs}}(Cm_{\text{bas\_sim}} + C_{\text{ano}})/Cm_{\text{bas\_sim}}, \qquad (4)$$

where $Cm_{\text{bas\_obs}}$ is the observed 30-yr monthly average for the 1971–2000 period; other nomenclature is analogous to Eq. (3).
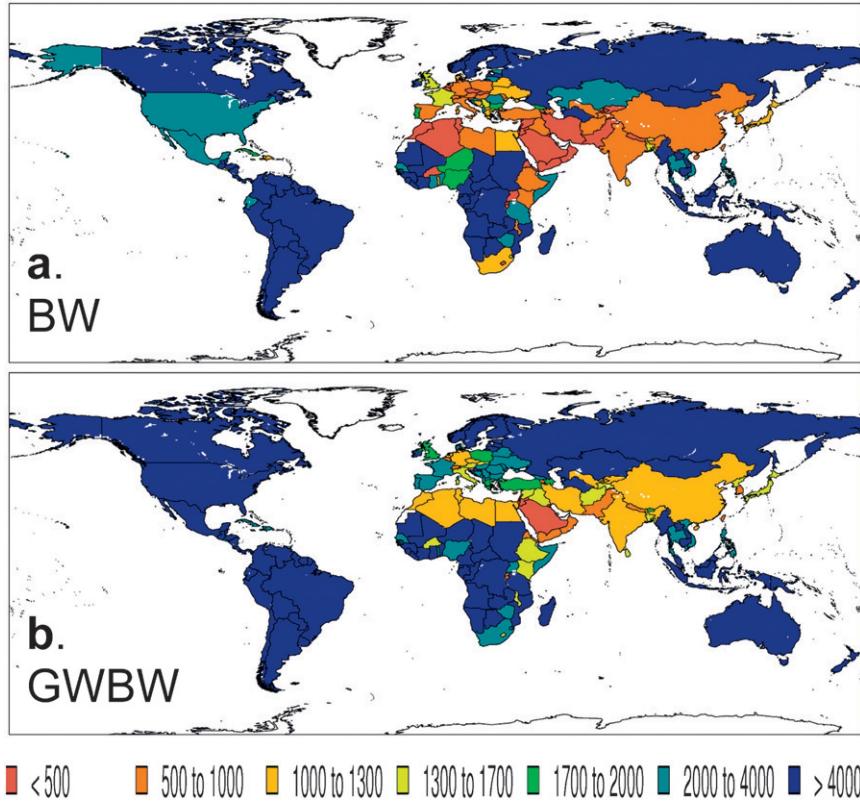
FIG. 2. Annual country-scale availability of (a) blue water and (b) green plus blue water in cubic meters per capita per year, averaged over the period 1971–2000.

If, by contrast, cloudiness is projected to increase ($C_{ano} > 0$), we assume

$$S_{scl} = Sm_{obs}(Sm_{bas\_sim} + S_{ano})/Sm_{bas\_sim}. \quad (5)$$

Here, S_{scl}, S_{ano}, etc. refer to the degree of cloudlessness [i.e., the inverse of cloudiness ($100 - C_{scl}$, $100 - C_{ano}$, etc.)]; all other nomenclature is analogous to Eq. (4).

For precipitation, a mixed additive-multiplicative approach was chosen that down-weights potentially very large relative increases in cases where GCMs underestimate observed precipitation [for a more detailed description of this methodology, see Füssel (2003)]:

$$P_{scl} = P_{obs}[1 + (P_{ano}/P_{bas\_obs})(P_{bas\_obs}/P_{bas\_sim})^{\lambda}], \quad (6)$$

where P_{bas_obs} is the observed 30-yr monthly average for the 1971–2000 period and the other variables are analogous to those in the above equations. The exponent λ is defined as the square root of $(P_{bas\_sim}/P_{bas\_obs})$ if $P_{bas\_sim} < P_{bas\_obs}$; otherwise it is 1.

Changes in the monthly number of wet days were not available from the GCMs, thus the values from the 1971–2000 baseline period were used. Annual atmospheric CO_2 concentrations until 2099 were taken from the Bern-CC carbon cycle model (see http://www.ipcc-data.org/ancilliary/tar-bern.txt).

To quantify the net physiological and structural effects of CO_2 concentration on plants and ultimately on the water scarcity indicator used here, we ran additional LPJmL simulations in which this concentration was held constant at its year 2000 level. Finally, we used population projections consistent with the emissions and climate projections (also at 0.5° resolution) to determine future per capita water availabilities. In the case of A2 we used the revised "A2r" scenario that shows lower population numbers than the original scenario (Grübler et al. 2007).

4. Results

a. Current water availabilities and requirements for food production

As illustrated in Fig. 2a, present-time BW availability per person is rather low (e.g., <1700 cubic meters per capita per year) not only in many physically water-poor countries in subtropical regions but also, for example, in Central Europe where population is dense. If the GW

resource is added (Fig. 2b), water availability becomes significantly higher in almost all regions, although a significant number of countries remain below 1700 cubic meters per capita per year (especially in North Africa and the Near East). By contrast, most countries at high latitudes and in the humid tropics, or countries with few resources but low population (such as Australia), are characterized by high per capita water availability (>4000 m^3).

In addition to water availability, we calculated the crop water requirements for producing the specified balanced diet from the grid cell-specific CFT fractions. Growing the equivalent of 1000 kcal of vegetal food on cropland—shown in Fig. 3a at grid cell level to enable localization of crop areas and identification of subnational variability—requires significantly more water in sub-Saharan Africa and in the Middle East (>1 m^3) than, for example, in most parts of Europe and in the United States/Canada (<0.5 m^3). Figure 3b shows that the resulting water requirements (including those for the livestock sector) for a balanced diet of 3000 kilocalories per capita per day also vary greatly among countries. According to these results, many countries in Europe and North America but also China and Egypt need less water to produce this diet than suggested by the global average (1095 cubic meters per capita per year; Fig. 1), whereas in other countries the respective water needs are much higher (often >2500 cubic meters per capita per year, especially in Africa). The regional pattern of the water needs results from differences in CWP, which in turn are controlled mainly by differences in climatic conditions, yield levels, and management intensity [for a detailed explanation of spatial patterns of CWP—or its inverse, the virtual water content—of maize and temperate cereals, see Fader et al. (2010), and especially their Figs. 2 and B1]. It was found that the yield level is often the prime factor determining CWP, as low values of CWP usually occur in regions with low yields, while low values of ET can still imply high yields (Fader et al. 2010).

b. Current water scarcity of countries

The present degree of water scarcity varies among countries according to their individual total water availability and their water requirements for producing a diet of 3000 kcal for their population (Fig. 3c). Note that many European countries that were classified as chronically water-scarce according to the Falkenmark indicator (see Fig. 2b) no longer appear to be water-scarce when our new indicator is used, since comparatively little water is needed there for producing a unit of crop (and livestock) (cf. Figs. 3a,b). Likewise, other countries that were classified as water-stressed in Fig. 2 (e.g., South Africa, China, Japan) actually have enough water to produce the specified diet. However, parts of

those countries would appear water-stressed if the analysis were done at subnational (grid cell) scale (not shown).

c. Future changes in water availability

Blue, green, and total water availabilities are simulated to change significantly in the future under the suite of climate models considered (Fig. 4). Patterns of change are different for BW and GW, and changes in water availabilities are generally stronger in either direction in the A2 scenario than in the B1 scenario. Country-scale BW availability will decrease in both scenarios—for instance, in southern Europe, the Near East (by $>40\%$ in some countries), northern and southern Africa, and Central America and Mexico, mostly in response to higher temperatures and regional precipitation decreases [data not shown, but see Bates et al. (2008)]. GW availability is simulated to decrease in most countries but Canada and central and northern Asia.

The regional pattern of relative change in GW and GWBW availability results from the complex interplay of impacts of changing precipitation, temperature, and CO_2 concentration (all of which affect potential ET and soil moisture—also on nonagricultural areas covered with PFTs with effects on BW availability), and also from CFT-specific shifts in growing periods. This clearly demonstrates that climate change will decrease overall freshwater resources in many regions, in particular where changes in GW and BW go into the same direction. The effect of CO_2 rise is rather small for both BW and GW (see Table 2 for the global effect). BW availability would be slightly lower than indicated in Figs. 4a and 4d if CO_2 concentration was held constant, due to higher transpiration and lower runoff than under increasing CO_2 concentration (cf. Gerten et al. 2008). Note that population changes were not considered in this analysis, but see section 4e for such an analysis and for probabilities of change given the 17 climate models.

d. Future changes in water requirements for producing the balanced diet

Climate change by the 2080s (without CO_2 effects) will in many regions increase the water requirements for producing the balanced diet on present cropland (as illustrated exemplarily for the vegetal part and for the A2 scenario in Fig. 5). This increase is attributable primarily to the higher evaporative demand induced by the warming. Additionally, biomass production will probably decrease in some regions (e.g., due to lower precipitation), requiring more water for producing the same amount of biomass and, ultimately, the required calories. In contrast to these findings, the water requirements are projected to decrease in parts of Europe, along the Mediterranean coastline of North Africa, in western
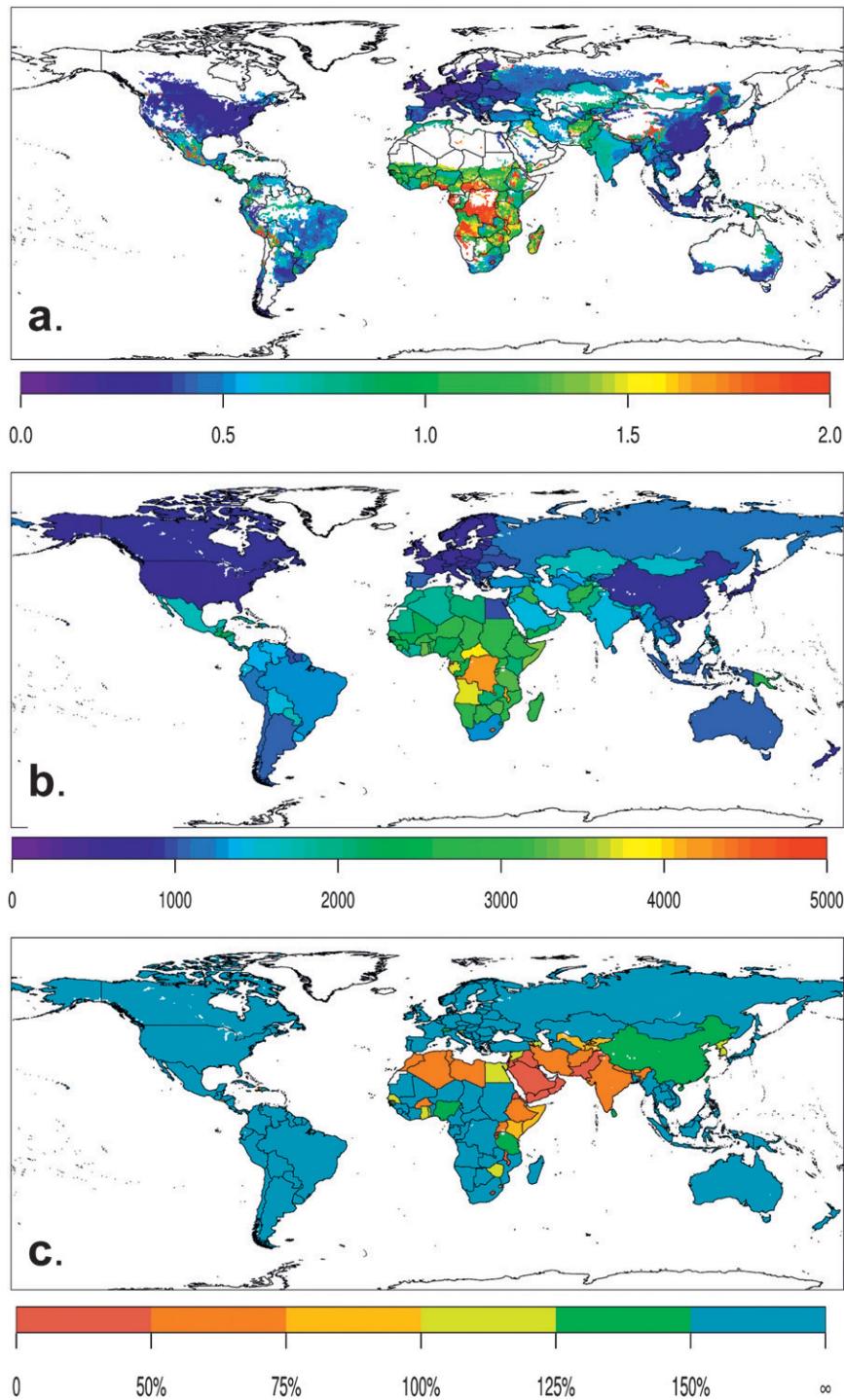
FIG. 3. GWBW requirements (m³, 1971–2000 average) for producing (a) 1000 kcal of vegetal food on cropland shown at gridcell level and (b) a daily diet of 3000 kcal with 80% vegetal and 20% animal products shown at country level. (c) Water scarcity defined as the percentage ratio between GWBW availability (cf. Fig. 2b) and the GWBW requirements for producing a daily diet of 3000 kcal from Fig. 3b. See text and Fig. 1 for calculation procedure.
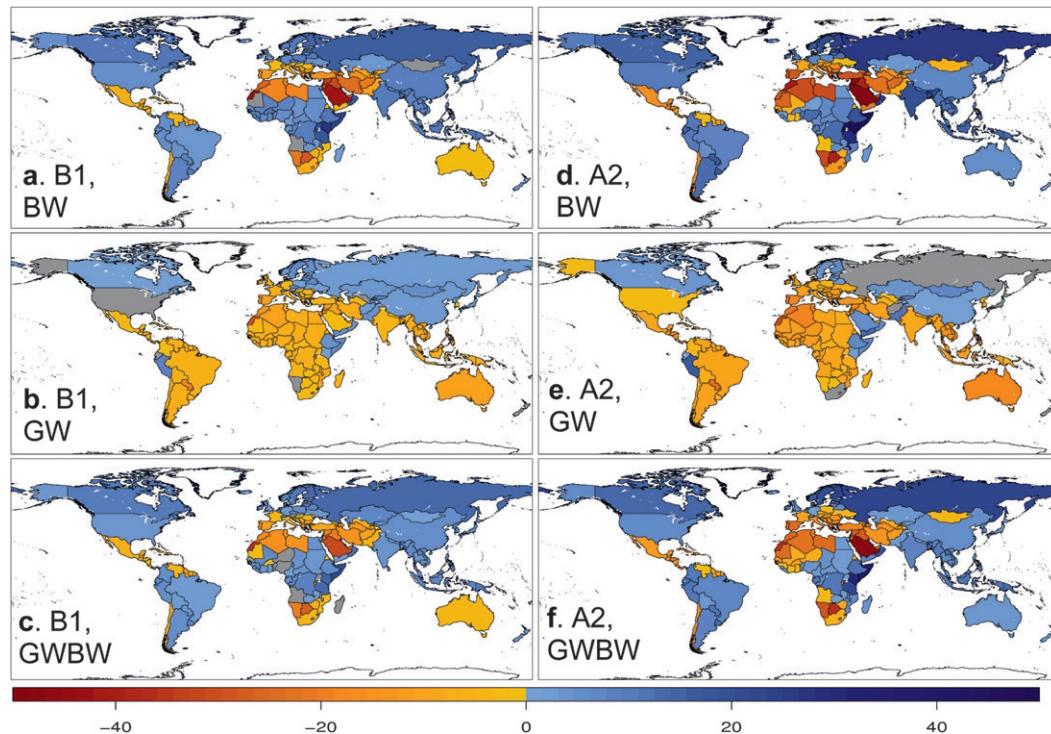
FIG. 4. Percent changes (medians across all climate scenarios, including CO_2 effects) in blue, green, and total water availability by the 2080s for B1 and A2 scenarios. Population held constant at year 2000 level (i.e., changes in water availability are equal to changes in water resources, and imposed only by changes in the climate). Gray colors indicate changes in the range of $0 \pm 0.5\%$.

Asia, and in southern Africa, where crop water productivity appears to increase. Increases and decreases for the B1 scenario—not shown here—are slightly less pronounced while exhibiting a spatial pattern similar to that for A2. See Fader et al. (2010) for individual responses of

crops to changes in climate and CO_2, which cannot be discussed in detail here.

It is important to note that the water requirements will decrease in most regions (sometimes by >20%) if the plant responses to the rising CO_2 concentration are

TABLE 2. Global numbers of people (in million, rounded) living in countries with water scarcity at present and in the 2080s under the B1 and A2 scenarios, both with and without population change. Water scarcity is defined both as the Falkenmark Index (GWBW availability <1300 cubic meters per capita per year) and as the failure to produce 3000 kilocalories per capita per day with the GWBW resources in a country (i.e., the new scarcity index developed herein). The values for the future represent the average across the 17 GCM projections ±one standard deviation to represent the variation across models. The population numbers are from the years 2000 and 2085, respectively.

Model period Scenario	1971–2000 CRU observed	2070–99 B1	2070–99 A2r
Climate and CO_2 change only			
Total population	6038	6038	6038
Water-stressed population (availability <1300 cubic meters per capita per year)	2966	2642 ± 596	2555 ± 665
Water-stressed population (availability less than requirements)	1671	1624 ± 19	972 ± 534
Climate and population change only			
Total population	6038	7877	11 998
Water-stressed population (availability <1300 cubic meters per capita per year)	2966	3375 ± 34	7786 ± 180
Water-stressed population (availability less than requirements)	1671	3640 ± 101	6878 ± 95
Climate, CO_2, and population change			
Total population	6038	7877	11 998
Water-stressed population (availability <1300 cubic meters per capita per year)	2966	3376 ± 38	7704 ± 148
Water-stressed population (availability less than requirements)	1671	3456 ± 75	6100 ± 274

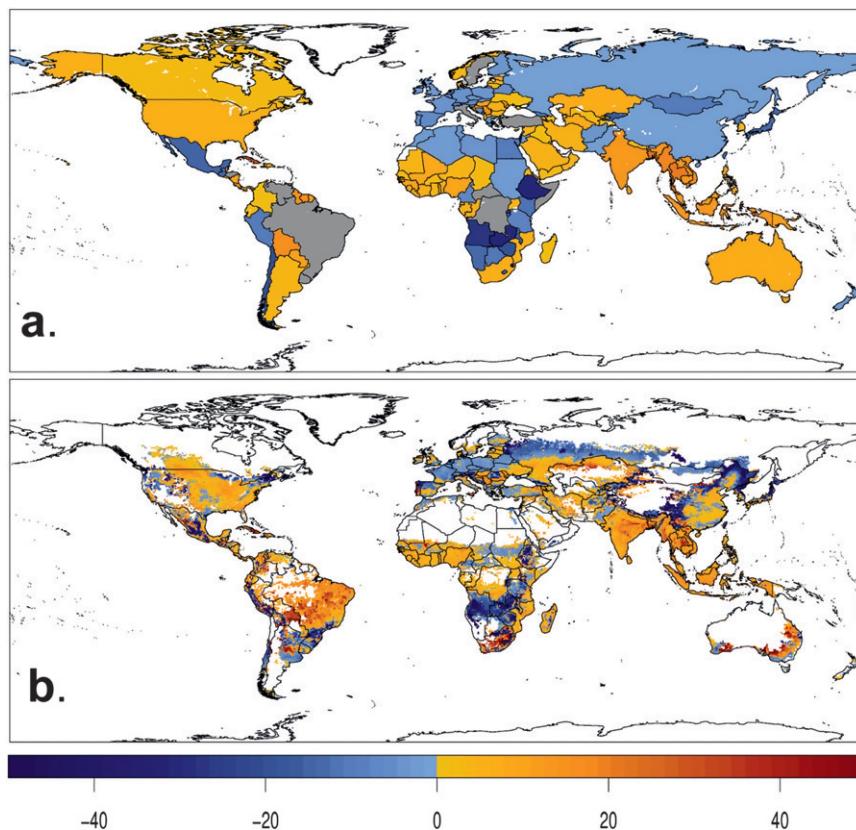FIG. 5. Climate-driven change in water requirements (%, median across all climate scenarios) for producing the vegetal part of the balanced diet on present cropland by the 2080s in the A2 scenario, shown (a) as country average and (b) at gridcell level, respectively. Effects of rising CO_2 concentration are not considered. Gray colors indicate changes in the range of $0 \pm 0.5\%$.

included (data not shown). As discussed below, however, the CO_2 effect simulated by LPJmL is a maximum effect unlikely to be fully realized under field conditions (see section 5).

e. Water scarcity under climate and population change

Figure 6a shows that given the whole spectrum of GCMs there is a high probability for many countries that per capita water availability will decline by at least 10% by the 2080s—this is particularly true for southern Europe and for northern and southern Africa (see also the ensemble median in Fig. 4f). However, the majority of countries in Asia are not projected to experience such a decline; and only very few countries that are presently not categorized as water-scarce are projected to become water-scarce (Fig. 6b). Interestingly, the global number of people living in countries whose GWBW resources will not be sufficient for producing 3000 kilocalories per capita per day—almost 1.7 billion presently—is projected to change little (in B1) or even to decline (in A2) by the

2080s in response to climate and CO_2 change (assuming present population) (Table 2). This is partly attributable to the beneficial CO_2 effect and partly to regional precipitation increases.

Given both climate and population change, however, there is a >90% probability that per capita water availability will decrease by 10% or more in most countries but eastern Europe and northern Asia (see Fig. 6c). Concurrently, countries in Africa, the Near East, and the Middle East that are presently water-scarce will remain in this state (cf. Figs. 6d and 3c). In addition, a number of countries that are presently capable to produce 3000 kcal day^{-1} for their inhabitants (e.g., Mali, Mauretania, and Angola) are very likely to lose this capacity by the 2080s, even though the underlying water requirements will decrease (see, e.g., Angola in Fig. 5). In contrast, most countries in the Americas and also Australia will on average still have enough green plus blue water resources for producing the specified diet, even though there is a high risk that water availability per person will decline by >10% in
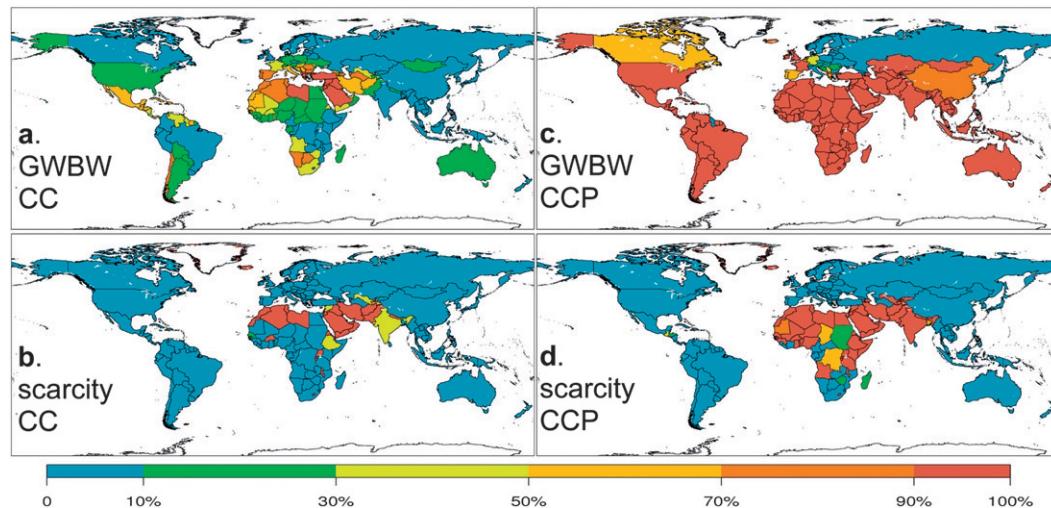
FIG. 6. Likelihood (%) of (a),(c) a reduction of GWBW availability by >10% by the 2080s and (b),(d) being water-scarce in the 2080s (left) under climate change only (CC; including CO_2 effects) and (right) under additional consideration of population change (CCP). Results are presented for the A2r scenario. The likelihoods were derived from the spread of impacts under all climate models [e.g., 90% means that the given impact occurs in 9 out of 10 (~15 out of 17) climate change projections].

most of these countries (Fig. 6c). If both climate and population change are accounted for, the global number of people living in water-scarce countries will rise to ~3.5 billion (B1) and ~6 billion (A2), respectively, meaning that the fraction of the global population living in water-scarce countries will rise from 28% at present to 43%–50% (A2) in the 2080s (Table 2).

Generally, the number of people living in water-scarce countries is lower if the new indicator is used instead of the fixed threshold of 1300 cubic meters per capita per year. Furthermore, as becomes evident by a comparison of Figs. 6b,d and 7a,b (also see Table 2), the effect of rising CO_2 concentration is quite small globally but significant in some countries, particularly in Africa and South Asia including India. (Figure 7c shows the effect of a reduced animal share of the required calorie uptake; see following section.)

f. Effect of the target diets' animal share

All above analyses are based on the assumption that the diet of 3000 kilocalories per capita per day contains 20% animal products. Since this diet can be composed of any meat share from a caloric point of view, we quantified the effect on water scarcity if this share was reduced to 10%. The direct comparison of Figs. 7c and 6d suggests that under this alternative assumption, less countries will be put at risk of being water-scarce in the future (e.g., Sudan and Congo will move out of this category), and for a number of other countries the likelihood of being water-stressed will decrease (e.g., from >90% to <70% in Egypt).

5. Discussion

This study represents an advancement in the development of a freshwater scarcity indicator that consistently compares per capita green and blue water availability to water requirements for food production, while considering dynamic changes in water availability and requirements as simulated by a global ecohydrological model. An application of this indicator demonstrates that applying a fixed threshold (such as 1300 cubic meters per capita per year; Rockström et al. 2009) may give a biased view on water constraints to food production in that it tends to overrate water scarcity (see Table 2). The reason is that due to differences in crop water productivity significantly more, or significantly less, water is actually required in individual regions to produce a given diet (such as the balanced diet of 3000 kilocalories per capita per day with 80% vegetal products, a benchmark for hunger alleviation).

Another major finding of this study is that water scarcity will aggravate in many countries, particularly in large parts of Africa and southwestern Asia. This worsening will be driven primarily by population growth and only secondarily by climate change (see Table 2), which principally agrees with findings from earlier studies based on blue water only (Vörösmarty et al. 2000; Arnell 2004). Even if GW is considered in addition to BW, water scarcity is projected to aggravate [as has already been indicated by Rockström et al. (2009) based on a limited set of climate and socioeconomic projections; see also Zehnder (2002) for a similar, albeit
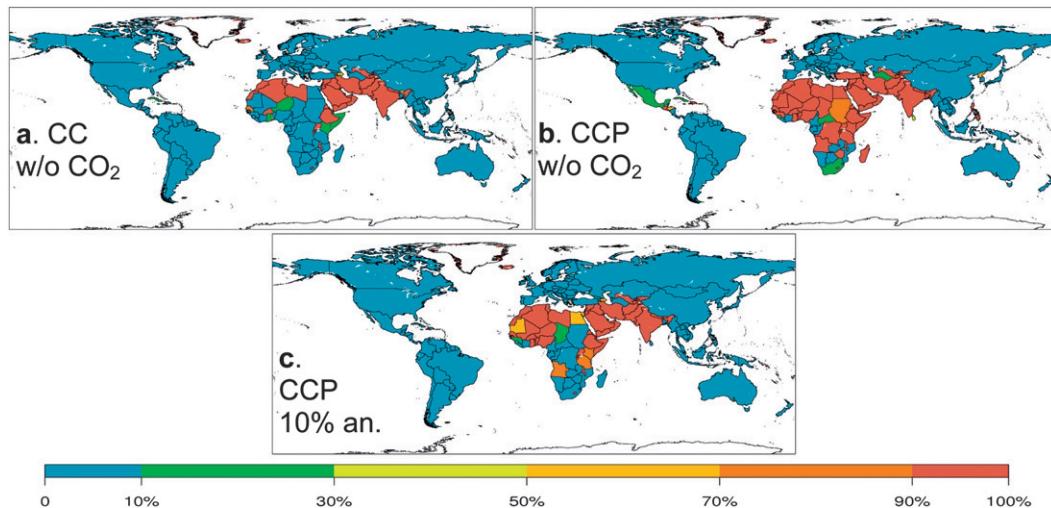
FIG. 7. Sensitivity analysis of the results shown in Figs. 6b and 6d regarding the likelihood of countries to be water-scarce in the 2080s: (a) only climate change with CO_2 effect excluded; (b) both population and climate change with CO_2 effect excluded; and (c) population, climate, and CO_2 change while assuming a halved calorie share from animal products only. Details are as in Fig. 6.

simpler analysis]. Note, however, that a small part of the underlying decrease in the GW resource is due to CO_2 rise, whose physiological effect decreases transpiration and whose structural effect increases biomass production and yields (Leipprand and Gerten 2006). This indicates that ET on cropland/grazing land is an ambiguous proxy for the GW resource, suggesting a worse water scarcity situation although yields can be increased. Further studies are required on the definition of the GW resource consistently with the BW resource—for example, by directly including plant water limitation in the indicator (Gerten et al. 2007; Rost et al. 2009)—and the sensitivity of results to these definitions. Also note that potential future land use changes and their effects on GW resources were not considered in this study. For example, the GW resource will be higher in countries where cropland or grazing land will be expanded in the future (e.g., as an option to adapt to the water shortage on present agricultural land). Such land use changes will affect the BW resource as well, usually by an increase in runoff (e.g., Gerten et al. 2008).

As discussed above, the present results include the beneficial ''more crop per drop'' effect of rising CO_2 concentration, which is a direct consequence of the higher CWP especially of C3 crops. However, the model used here implicitly assumes the absence of nutrient limitation—hence, the simulated CO_2 effect is at a maximum that is unlikely to be realized especially in low-managed systems, unless comprehensive measures are taken to surmount nutrient limitations and other limiting factors such as pests and diseases. Moreover, crops grown under higher CO_2 concentration may have

a lower quality as food (e.g., Bloom et al. 2010), which would increase the amount of water needed to produce the required calories. Conversely, improved water and soil management in irrigated and rain-fed systems—for example, increases in the fraction of productive transpiration by reducing soil evaporation, or crop breeding—could augment CWP more than projected here [see Rost et al. (2009) for a global quantification of such management changes]. A caveat of this study is that crop management is held constant for the future; anticipated management changes will have to be incorporated into an upcoming version of the LPJmL model. Effects of theoretical management improvements in relation to effects of climate change are being analyzed in an ongoing study (J. Heinke 2011, personal communication).

In general, the GWBW availability found herein is somewhat lower compared to the findings by Rockström et al. (2009; see their Fig. 7a). This may be partly attributable to differences in the climate and land use datasets used, but the prime reason is that the BW and the GW resources were defined more conservatively in this study [Rockström et al. (2009) reduced the BW resource by only 30% and accounted for 100% of year-round ET from grazing land]. Similar to the above discussion on GW, this points to the fact that the exact definition of BW (including the proportion that is actually accessible after subtraction of, e.g., environmental flows and high flows)—and also the spatial scale at which water availability and population are compared (see Vörösmarty et al. 2000)—co-determine whether a region or country is classified as being water-scarce. Moreover, possible water scarcity at subnational scale

and in individual years and/or seasons is masked by the long-term annual averages presented in this study. Further systematic investigations will have to be made at various temporal and spatial resolutions (e.g., focused on impacts of dry spells and droughts due to increasing climate variability and extremes), with variants of definitions of the GW and BW resource, and with different assumptions about the scale at which the food is distributed.

The focus of the water scarcity indicator developed here is on water (available on present cropland) for food self-sufficiency of countries (as in Rockström et al. 2007, 2009), assuming that people's diets are based only on domestically produced vegetal and animal commodities. Therefore, an imperative next step toward a more complete account of water limitations to food security will be to consider the income levels (affecting the capacity to implement water-saving technologies, the food demand/diet composition, etc.), different compositions of the target diet, and the origin of the consumed products if there is no food self-sufficiency and countries import food from other countries. Effects of a different share of vegetal and animal products were quantified in this study (Fig. 7), indicating that eating fewer animal products eases the water scarcity situation. This preliminary result should be regarded as a sensitivity analysis rather than a projection, because (i) it is simply assumed here that eight times more water is needed to produce animal calories than to produce vegetal food (while in reality this value differs among production systems), (ii) water consumption in the livestock sector is treated crudely in the present analysis, and (iii) meat consumption and related feedstuff production probably will increase significantly in a number of countries (e.g., due to urbanization processes). The 20% share of animal products assumed in this study implies such an increase in, for instance, African countries (where the present share is <10%) but a decrease in the United States and Europe (presently 25%–30%; see, e.g., Rockström et al. 2005).

These research tasks will require a more detailed account of the water requirements for livestock products (e.g., by considering livestock feed baskets) and ultimately an integration of virtual water trade (see, e.g., Chapagain and Hoekstra 2008) by accounting for the actual and potential future global pattern of production and consumption of agricultural products together with the underlying green and blue freshwater resources. Nonetheless, this study represents a major step toward a more comprehensive and spatially explicit assessment of the water needs and limitations for producing the food (calories) for a growing world population.

REFERENCES

Alcamo, J., M. Flörke, and M. Marker, 2007: Future long-term changes in global water resources driven by socio-economic and climatic changes. *Hydrol. Sci. J.,* **52,** 247–275.

Arnell, N. W., 2004: Climate change and global water resources: SRES emissions and socio-economic scenarios. *Global Environ. Change,* **14,** 31–52.

Bates, B. C., Z. W. Kundzewicz, S. Wu, and J. P. Palutikof, Eds., 2008: Climate change and water. IPCC Tech. Paper VI, 210 pp.

Biemans, H., R. Hutjes, P. Kabat, B. Strengers, D. Gerten, and S. Rost, 2009: Effects of precipitation uncertainty on discharge calculations for main river basins. *J. Hydrometeor.,* **10,** 1011–1025.

——, I. Haddeland, P. Kabat, F. Ludwig, R. W. A. Hutjes, J. Heinke, W. von Bloh, and D. Gerten, 2011: Impact of reservoirs on river discharge and irrigation water supply during the 20th century. *Water Resour. Res.,* **47,** W03509, doi:10.1029/2009WR008929.

Bloom, A. J., M. Burger, J. S. R. Asensio, and A. B. Cousins, 2010: Carbon dioxide enrichment inhibits nitrate assimilation in wheat and Arabidopsis. *Science,* **328,** 899–903.

Bondeau, A., and Coauthors, 2007: Modelling the role of agriculture for the 20th century global terrestrial carbon balance. *Global Change Biol.,* **13,** 679–706.

Chapagain, A. K., and A. Y. Hoekstra, 2008: The global component of freshwater demand and supply: An assessment of virtual water flows between nations as a result of trade in agricultural and industrial products. *Water Int.,* **33,** 19–32.

Fader, M., S. Rost, C. Müller, and D. Gerten, 2010: Virtual water content of temperate cereals and maize: Present and potential future patterns. *J. Hydrol.,* **384,** 218–231.

——, D. Gerten, M. Thammer, J. Heinke, H. Lotze-Campen, W. Lucht, and W. Cramer, 2011: Internal and external green-blue agricultural water footprints of nations, and related water and land savings through trade. *Hydrol. Earth Syst. Sci.,* **15,** 1641–1660.

Falkenmark, M., J. Rockström, and L. Karlberg, 2009: Present and future water requirements for feeding humanity. *Food Secur.,* **1,** 59–69.

FAO, 2003: *World Agriculture: Towards 2015/2030—An FAO Perspective.* Earthscan, 432 pp.

Füssel, H.-M., 2003: Impact analysis for inverse integrated assessments of climate change. Ph.D. thesis, Potsdam University, 178 pp.

Gerten, D., S. Schaphoff, U. Haberlandt, W. Lucht, and S. Sitch, 2004: Terrestrial vegetation and water balance: Hydrological evaluation of a dynamic global vegetation model. *J. Hydrol.,* **286,** 249–270.

——, ——, and W. Lucht, 2007: Potential future changes in water limitation of the terrestrial biosphere. *Climatic Change,* **80,** 277–299.

——, S. Rost, W. von Bloh, and W. Lucht, 2008: Causes of change in 20th century global river discharge. *Geophys. Res. Lett.,* **35,** L20405, doi:10.1029/2008GL035258.

Grübler, A., and Coauthors, 2007: Regional, national, and spatially explicit scenarios of demographic and economic change based on SRES. *Technol. Forecast. Soc.,* **74,** 980–1029.

Haddeland, I., and Coauthors, 2011: Multimodel estimate of the global terrestrial water balance: Setup and first results. *J. Hydrometeor.,* **12,** 869–884.

Hoff, H., M. Falkenmark, D. Gerten, L. Gordon, L. Karlberg, and J. Rockström, 2010: Greening the global water system. *J. Hydrol.,* **384,** 177–184.

Islam, S., T. Oki, S. Kanae, N. Hanasaki, Y. Agata, and K. Yoshimura, 2007: A grid-based assessment of global water scarcity including virtual water trading. *Water Resour. Manage.,* **21,** 19–33.

Lannerstad, M., 2009. Water realities and development trajectories: Global and local agricultural production dynamics. Ph.D. thesis, Linköping University, 123 pp.

Leipprand, A., and D. Gerten, 2006: Global effects of doubled atmospheric CO_2 content on evapotranspiration, soil moisture and runoff under potential natural vegetation. *Hydrol. Sci. J.,* **51,** 171–185.

Liu, J. G., J. R. Williams, A. J. B. Zehnder, and H. Yang, 2007: GEPIC—Modelling wheat yield and crop water productivity with high resolution on global scale. *Agric. Syst.,* **94,** 478–493.

——, A. J. B. Zehnder, and H. Yang, 2009: Global consumptive water use for crop production: The importance of green water and virtual water. *Water Resour. Res.,* **45,** W05428, doi:10.1029/2007WR006051.

Mann, M. E., 2004: On smoothing potentially nonstationary climate time series. *Geophys. Res. Lett.,* **31,** L07214, doi:10.1029/2004GL019569.

Mitchell, T. D., and P. D. Jones, 2005: An improved method of constructing a database of monthly climate observations and associated high-resolution grids. *Int. J. Climatol.,* **25,** 693–712.

Molden, D., Ed., 2007: *Water for Food Water for Life: A Comprehensive Assessment of Water Management in Agriculture.* Earthscan, 665 pp.

Portmann, F. T., S. Siebert, and P. Döll, 2010: MIRCA2000—Global monthly irrigated and rainfed crop areas around the year 2000: A new high-resolution data set for agricultural and hydrological modeling. *Global Biogeochem. Cycles,* **24,** GB1011, doi:10.1029/2008GB003435.

Ramankutty, N., A. T. Evan, C. Monfreda, and J. A. Foley, 2008: Farming the planet: 1. Geographic distribution of global agricultural lands in the year 2000. *Global Biogeochem. Cycles,* **22,** GB1003, doi:10.1029/2007GB002952.

Randall, D. A., and Coauthors, 2007: Climate models and their evaluation. *Climate Change 2007: The Physical Science Basis,* S. Solomon et al., Eds., Cambridge University Press, 589–662.

Rockström, J., G. N. Axberg, M. Falkenmark, M. Lannerstad, A. Rosemarin, I. Caldwell, A. Arvidson, and M. Nordström, 2005: *Sustainable Pathways to Attain the Millennium Development Goals: Assessing the Key Role of Water, Energy and Sanitation.* Stockholm Environment Institute, 106 pp.

——, M. Lannerstad, and M. Falkenmark, 2007: Assessing the water challenge of a new green revolution in developing countries. *Proc. Natl. Acad. Sci. USA,* **104,** 6253–6260.

——, M. Falkenmark, L. Karlberg, H. Hoff, S. Rost, and D. Gerten, 2009: Future water availability for global food production: The potential of green water for increasing resilience to global change. *Water Resour. Res.,* **45,** W00A12, doi:10.1029/2007WR006767.

Rost, S., D. Gerten, A. Bondeau, W. Lucht, J. Rohwer, and S. Schaphoff, 2008: Agricultural green and blue water consumption and its influence on the global water system. *Water Resour. Res.,* **44,** W09405, doi:10.1029/2007WR006331.

——, ——, H. Hoff, W. Lucht, M. Falkenmark, and J. Rockström, 2009: Global potential to increase crop production through water management in rainfed agriculture. *Environ. Res. Lett.,* **4,** 044002, doi:10.1088/1748-9326/4/4/044002.

Schuol, J., K. C. Abbaspour, H. Yang, R. Srinivasan, and A. J. B. Zehnder, 2008: Modeling blue and green water availability in Africa. *Water Resour. Res.,* **44,** W07406, doi:10.1029/2007WR006609.

Siebert, S., and P. Döll, 2010: Quantifying blue and green virtual water contents in global crop production as well as potential production losses without irrigation. *J. Hydrol.,* **384,** 198–217.

Vörösmarty, C. J., P. Green, J. Salisbury, and R. Lammers, 2000: Global water resources: Vulnerability from climate change and population growth. *Science,* **289,** 284–288.

Waha, K., L. G. J. van Bussel, C. Müller, and A. Bondeau, 2011: Climate-driven simulation of global crop sowing dates. *Global Ecol. Biogeogr.,* in press.

Weiß, M., R. Schaldach, J. Alcamo, and M. Flörke, 2009: Quantifying the human appropriation of fresh water by African agriculture. *Ecol. Soc.,* **14,** 25. [Available online at http://www.ecologyandsociety.org/vol14/iss2/art25/.]

Zehnder, A. J. B., 2002: Wasserressourcen und Bevölkerungsentwicklung. *Nova Acta Leopoldina NF 85,* **323,** 399–418.